Effects of Turbulence on the Drag Coefficients of Spheres in a Supercritical Flow Regime

ALLEN CLAMEN and W. H. GAUVIN

McGill University, Montreal, Quebec, Canada
and Pulp and Paper Research Institute of Canada, Montreal, Quebec, Canada

Drag coefficients of aerodynamically smooth spheres varying in diameter from 0.0625 to 1.004 in. and in density from 0.195 to 7.80 g./cc. were obtained at acceleration rates ranging from 120 to —30 ft./sq.sec. The particles were subjected to relative turbulence intensities of 7 to 35% and to ratios of Eulerian macroscale to particle diameter of about 0.4 to 5.

Quantitative measurement of particle drag coefficients was made possible by the use of a new particle tracing technique which permits the resolution of time to the nearest tenth of a millisecond. The resulting data extend farther into the supercritical flow regime than any other measurements previously reported.

The variation in drag coefficient with Reynolds number indicates a continuous alteration in the flow pattern around a sphere in this region. The effect of turbulence is, essentially, to increase supercritical drag, although this effect was found to diminish with increasing Reynolds number. Possible mechanisms for the effects of Reynolds number and turbulence on the particle drag coefficient are suggested.

Practical engineering applications involving the intimate contact between solid particles and a continuous fluid medium are being developed at a rapidly growing rate. These systems, in general, play an important role in a large variety of industrial operations, such as pneumatic conveying, transport reactions, spray processes, flash drying, air pollution control, and the design of solids-burning rocket engines. Although empirical relationships have been derived to determine the rates of heat, mass, and momentum transfer in solids-gas flow under certain conditions, the basic principles underlying the behavior of particulate systems are still, to a large extent, imperfectly understood. In particular, the effects of a number of important factors on the motion of a particle conveyed by a moving fluid still remain to be assessed. One such effect is the influence of the level of free-stream turbulence on the fluid resistance to particle motion.

BOUNDARY LAYER TRANSITION CAUSED BY TURBULENCE

Free-stream turbulence is known to exert a significant influence on the momentum transfer from a particle by altering the flow field around it. The best known of these alterations is the transition in the attached boundary layer from laminar to turbulent flow. This action is responsible for the major effect of free-stream turbulence, namely the lowering of the critical Reynolds number, defined by convention as that value of N_{Re} at which the declining steeply sloped portion of the C_D — N_{Re} curve intersects the C_D value of 0.3 (*1*). By promoting transition, the essential effect of an increase in the intensity of free-stream turbulence is to influence the position of boundary layer separation. The latter determines the size of the wake which, in turn, has a dominating influence on the drag of a sphere.

The form of the dependence of N_{Re_c} on the intensity of turbulence in the main stream has been found by Torobin and Gauvin (*1*) in their study of the effects of turbulence on the drag coefficients of spheres. By injecting spherical particles into a cocurrent turbulent stream and measuring their subsequent time-distance history, they were able to show that the critical Reynolds number can be as low as 400 if the relative intensity is high enough. The effect of turbulence on particle motion was characterized by the relative intensity I_R, defined as $\sqrt{\overline{u'^2}}/U$, where U is the relative velocity between the particle and the fluid. The experimental results of Torobin and Gauvin supported their transition theory which predicted that:

$$(N_{Re_c})(I_R^2) = K \rightarrow (N_{Re_c})(I_R^2) = K \qquad (1)$$

where K was found experimentally to be 45 for spheres.

EFFECTS OF TURBULENCE ON PARTICLE FLOW FIELD

Boundary-layer transition alone does not account for all the changes in transport phenomena observed in the presence of free-stream vorticity. The laminar and turbulent boundary layers and the separated region behind a particle have all been observed to respond in some measure to the influence of free-stream turbulence.

In 1935, Hoerner (*2*) noticed that the supercritical drag on a sphere is increased by turbulence and suggested that this increase may be due to apparently intensified viscosity. More recently, large increases (300%) in the skin friction of a turbulent boundary layer have been revealed for a flat plate (*3*) in the presence of external turbulence of 20% intensity. The contribution of shear stress to the drag on a sphere is, however, minor at supercritical Reynolds numbers.

More important is the effect of turbulence on the position of separation and the size of the wake behind a sphere. Concerning the former effect, Wadsworth (*4*), in a study of the influence of turbulence on heat transfer, observed that an increase in free-stream turbulence caused the separation circle on a sphere to move only a few degrees down stream. This displacement is believed to be too slight to have altered the drag significantly. Concerning wake size, Ahlborn (*5*), in a series of photographs of the wake behind a cylinder, showed vividly the stunting of the wake by the direct action of turbu-

A. Clamen is with Esso Research & Engineering Co., Linden, New Jersey and W. H. Gauvin is with Noranda Research Centre, Pointe Claire, Quebec, Canada.

lence. In this regard, results for flat plates in the normal orientation, where the point of separation is fixed and only changes in wake structure can affect C_D, shows a steady rise in drag coefficient with free-stream turbulence intensity (*6*).

VARIATION OF DRAG COEFFICIENT IN SUPERCRITICAL REGIME

Although many industrial processes involve the motion of a spherical particle in supercritical flow, there is very little information available in the literature regarding the variation of drag coefficient with Reynolds number in this regime. For a sphere, only the work of Jacobs (*7*) has provided data for the $C_D - N_{Re}$ relationship at $N_{Re} > 10^6$. He found the reduction in drag following transition to be followed by a gradual increase up to $N_{Re} = 10^7$. Beyond this value, Hoerner (*8*) has predicted another decrease in C_D for the sphere or cylinder due to the decreasing values of the skin-friction coefficient.

In the absence of significant data regarding the motion of a sphere at high Reynolds numbers, insight may be gained from the studies of drag and wake shedding on a circular cylinder under similar conditions. In this respect, the works of Relf and Simmons (*9*), Delany and Sorensen (*10*), Drescher (*11*), Fung (*12*), and particularly Roshko (*13*) give experimental data on shedding frequencies or drag coefficients in the supercritical regime. Since the measurement of the Strouhal number is generally much more accurate than that of C_D, there are more data available for shedding frequencies. It has been known, moreover, that an increase in shedding frequency is accompanied by a decrease in drag, and vice versa (*9*). A better prediction of the behavior of C_D with respect to N_{Re} can thus be obtained by inference from the more complete $N_{St} - N_{Re}$ relationships available.

Probably the most important work to date on the flow past a bluff body at very high Reynolds number is that of Roshko (*13*). Utilizing a pressurized wind tunnel, he has investigated the N_{Re} range of 10^6 to 10^7 under essentially incompressible conditions. Roshko noted that, between N_{Re} of 10^6 and 3.5×10^6, the flow pattern around a cylinder undergoes a major change, which he terms the upper transition, ranking in magnitude with the change occurring in the lower or critical transition region $2 \times 10^5 < N_{Re} < 5 \times 10^5$. Following the upper transition is a regime of fairly constant behavior for $N_{Re} > 4 \times 10^6$, referred to as the *transcritical region*, where C_D reaches a plateau at a mean value of 0.70. Roshko suggested that a similar effect of turbulence should be expected on the upper transition as on the lower transition, namely that of lowering the critical N_{Re} at which it occurs.

EXPERIMENTAL

In order to obtain accurate drag-coefficient data for spheres moving in the presence of relatively high levels of free-stream turbulence, it is necessary to inject, or otherwise entrain, particles in a turbulent air stream at velocities close to that of the main flow. For this purpose, use was made of the turbulent-flow ballistics facilities developed originally by Torobin and Gauvin (*14*), and modified by Marchildon (*15*). A more accurate method of particle tracking was devised so as to obtain the time-distance history of the particle with the required accuracy.

Facilities for Particle Motion Studies in Turbulent Air

The system used in this investigation consisted of an 8 in. diameter, 20 ft. high, upward-flow wind tunnel with a turbulence-generating grid system at the inlet. A particle injector operated by compressed air was located at the tunnel entrance and served to impel single spherical particles at a predetermined velocity along the center-line of the tunnel, and in a nonrotating manner. A schematic diagram of the wind tunnel and associated equipment is shown in Figure 1. More detailed information concerning the main components of the turbulent flow ballistics facilities can be found elsewhere (*14*).

Particle Injection

The particle launching device consisted of a gun barrel or vertical steel tube with a sabot or piston accurately fitted to travel smoothly up the barrel. The sabot was constructed of nylon and protected from impact fracture with an aluminum sleeve. The test sphere rested in a conical depression on top of the sabot.

The sabot was propelled up the barrel by a blast of compressed air (from a reservoir) entering on both sides of the barrel. An annular arresting plate located at the top of the gun barrel served to stop the sabot while allowing the particle to continue unimpeded into the turbulent air stream. With proper alignment, it was possible to fire spheres directly along the tunnel axis for its entire length.

Turbulence Characteristics of Air Stream

The gun barrel extended into the tunnel entrance through a series of orifice grids which were housed in a vertical stack of converging rings. This turbulence-generating system is identical to that described in the literature (*14*).

A careful study was made of the turbulence characteristics of the flow in the wind tunnel resulting from this generating system. With the use of a constant-current hot-wire anemometer, the absolute longitudinal intensity was measured at seven points along the axis. These measurements were repeated using a constant-temperature anemometer, which indicated that the previous results were slightly low at all locations, and particularly near the inlet. At the time of their experiments, however, Torobin and Gauvin (*1*) were aware that the values of turbulence intensity close to the inlet were somewhat lower than expected from theoretical considerations. Hence, although the data obtained in this region were not accepted by those authors, they were used in this investigation. The variation in turbulence intensity along the axis of the tunnel, as obtained with both anemometers, is shown in Figure 2.

The hot-wire anemometer was also used to obtain a profile across the tunnel of the longitudinal intensity at three locations, and the radial intensity at three points on the axis. The energy spectrum of turbulence fluctuations was also determined at various distances along the axis of the tunnel. From the measurements taken, it was evident that a nonperiodic spectrum was established very soon downstream from the grid inlet.

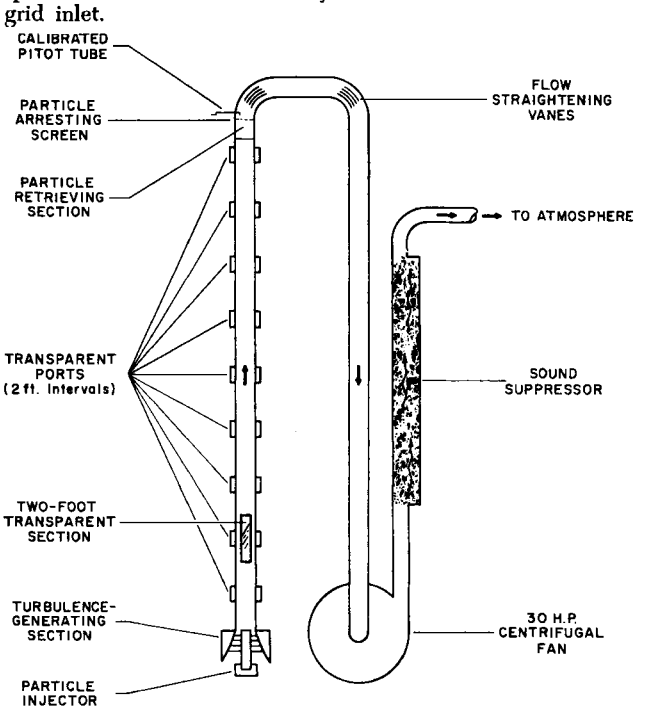

Fig. 1. Turbulent flow particle ballistics facility.

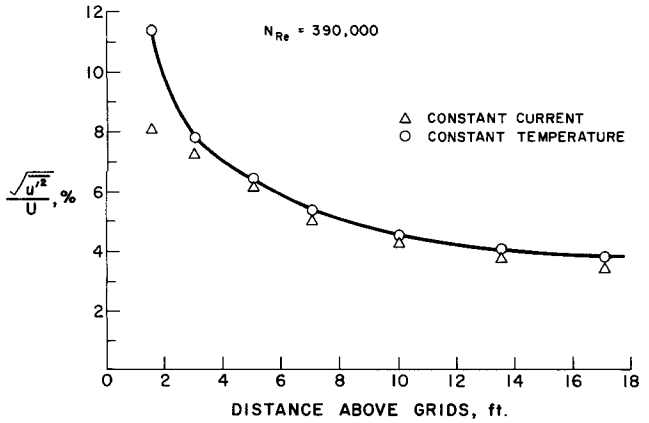

Fig. 2. Variation of turbulence intensity values along tunnel axis.

The correlation coefficient R_y for longitudinal velocity fluctuations was determined with a moveable head two-wire probe. From the area under the curve, obtained by plotting R_y against the radial separation distance, the Eulerian macroscale L was found to be 0.41 in., 0.41 and 0.34 in. at distances above the grids of 3, 10, and 17 ft., respectively. The microscale λ in the y direction was estimated to be 0.025, 0.017, and 0.015 in. for the three stations, respectively. It was apparent from the estimated values of microscale in the x and y direction that the turbulence throughout the tunnel was essentially isotropic.

To determine the air speed at the instant of firing, a calibrated pitot tube, which in turbulent flow provides a value intermediate between the root mean square and mean velocity, was installed just above the test section and connected to a manometer located near the particle injector. As a result, the uncertainty in air velocity was reduced from ± 1% to about ± 0.2%. By so doing, it was possible to obtain drag coefficients at very high values of I_R with increased accuracy.

Particle Tracking System

The main components of the apparatus used to obtain an accurate knowledge of the particle velocity history have been described elsewhere (*16, 17*). In essence, the tracking method consisted of measuring the time at which a particle interrupted a beam of light focused at the axis of the wind tunnel and shining on each of a series of nine photocells spaced at 2 ft. intervals. This was accomplished by recording the voltage pulses emitted by the photocells by means of an oscilloscope or of an optical oscillograph. Photographs of the oscilloscope screen were measured using a projection microscope equipped with a calibrated stage, while the Visicorder Optical Oscillograph traces were analyzed on a digitizing system. Both these methods permitted resolution of time to the nearest tenth of a millisecond, thus providing very accurate time-distance data. This precision made it possible to make reliable, quantitative measurements of the second derivatives of the particle trajectories and thus of the sphere drag coefficients.

RESULTS

The experimental facilities and technique described above were employed to provide a complete velocity history, including instantaneous values of the relative velocity U between the particle and the entraining air stream and of particle acceleration $\dot{U}_p$, for spheres under varying conditions of air turbulence. Only aerodynamically smooth spheres (which may be defined as those which have surface proturberances no greater than the boundary layer thickness) were employed, and the latter varied in density from 0.199 to 7.80 g./cc. and in diameter from 0.0625 to 1.004 in. The particles were injected singly at different velocities along the central axis of the wind tunnel into a cocurrent airstream of about 104 ft./sec. velocity. As a result, the spheres experienced acceleration rates of 120 to −30 ft./sq. sec. and were subjected to relative turbulence intensities of 7 to 35%. Several particle firings were carried out with the tunnel operating at approximately 75 ft./sec. The variation in turbulence intensity, therefore, was checked at this velocity and found to approximate the calibration obtained at the higher flow rate, as shown in Figure 2.

Drag coefficients were calculated over the entire length of the wind tunnel using the following equation derived from a momentum balance of the system:

$$C_D = 2(\dot{U}_p + g)m/\rho U^2 A_p \qquad (2)$$

From a knowledge of the variation in turbulence intensity I along the tunnel axis, the value of relative intensity I_R could be found at any point along the particle trajectory by the following relationship:

$$I_R = \sqrt{\overline{u'^2}/U} = (\sqrt{\overline{u'^2}/U_o})(U_o/U) = I(U_o/U) \qquad (3)$$

where U_o is the mean velocity of the air stream at the centerline of the wind tunnel.

Originally, sixty-six runs were performed with five photocells spaced accurately at 6 in. vertical intervals alongside the tunnel, with the bottom photocell about 2.5 ft. above the top of the injection device. The information obtained with this tracking system was processed by an IBM 1620 program which fitted the time-distance data to a second-order polynominal. As a result, a single average value of $\dot{U}_p$ was obtained. This gave an average C_D corresponding to the particle Reynolds number $N_{Re} = (DU\rho/\mu)$ and to the relative intensity of turbulence occurring at the central photocell. This simplification resulted from the fact that over the relatively short tracking distance employed (2 ft.), most particles experienced a negligible change in acceleration. Consequently the data could be fitted by the method of least squares using the following time-distance relation:

$$\theta = a + bx + cx^2 \qquad (4)$$

where, at the central photocell, $x = 0$, $U_p = 1/b$ and $\dot{U}_p = -2c/b^3$. The use of such a low order polynomial had the added benefit of smoothing out small errors in time and distance measurements. The maximum possible error $E(C_D)$ is given by the following expression:

$$E(C_D) = (k\rho_P D)(U_p/U)^2 \qquad (5)$$

where the constant k incorporates the possible relative error in the measurement of the distance between photocells (± 0.26%) and the error in time measurements (about ± 0.20%). From Equation (5) it is obvious that the use of small, low density particles injected at low velocities involved the least error. However, to obtain drag coefficient data over a range of Reynolds numbers

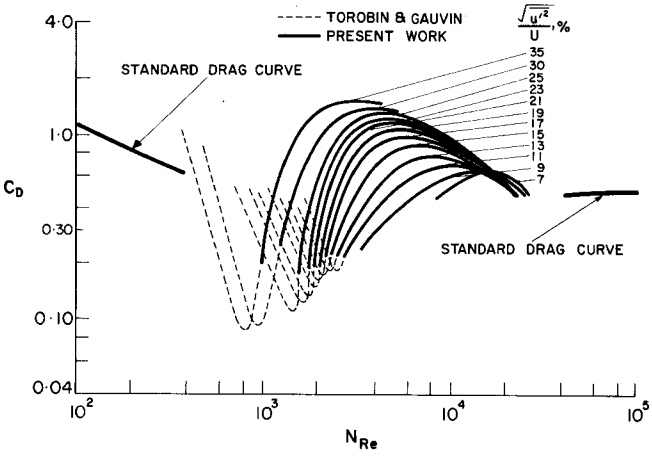

Fig. 3. Effect of relative intensity on the drag coefficients of spheres.

and relative turbulence intensities in the supercritical flow regime, it was necessary to employ, at times, sphere diameters as large as 1 in. and injection velocities close to that of the air stream. Nevertheless, low density particles were used, whenever possible, to maintain a high degree of accuracy. In this regard, it was found that small diameter particles of low density, because of their low inertia, tended to assume a fluctuating motion of their own, particularly at very high relative intensities of turbulence. Consequently, the data obtained with these spheres, in general, were not included in the results.

In order to take advantage of the high turbulence levels in the wind tunnel without incurring too large an error, it was necessary to obtain accurate point values of particle acceleration at various stations rather than average values over short sections of the tunnel. Consequently, nine photocells spaced at 2 ft intervals were employed as described in the previous section, and 173 additional runs were carried out. Under these conditions, acceleration could no longer be assumed to remain constant over the particle trajectory (16 ft.) and a higher order polynomial had to be used to fit the time-distance data. The computer results indicated that the data were accurately fitted without further smoothing by a third-order polynomial. The resulting $C_D - N_{Re}$ curves for values of I_R from 7 to 35% are shown in Figure 3.

In spite of the precision of the present data, considerable scatter was obtained which made it necessary to perform numerous experiments under similar conditions in order to obtain reliable average values of the drag coefficients. There appears to be some randomness associated with the flow field in the supercritical regime making reproduction of data possible on an average basis only. Experimental data and calculated results are shown in Table 1.*

DISCUSSION OF RESULTS

Although no study has been made of the changes in flow pattern around a sphere in the supercritical region, a great deal may be deduced from the dependence of the drag coefficient on the particle Reynolds number in this flow regime. The fact that the $C_D - N_{Re}$ curves obtained in this investigation are continually changing in slope and direction indicates a gradual alteration in flow pattern, beginning with the well known transition which occurs at the critical Reynolds number. This view is confirmed by the work of Roshko (*13*), who observed a similar variation in C_D with N_{Re} for cylinders. Formerly, it had been advanced that, at subcritical Reynolds numbers, the separation was laminar and occurred at a point near the equator of the sphere; as the Reynolds number was increased beyond N_{Re_c}, transition occurred in the attached boundary layer, upstream of the separation point. By inception of transition, the now turbulent boundary layer increased its energy slightly and hence was able to resist the adverse pressure gradient for a little farther around the surface of the sphere before separating. This description may account for the sudden decrease in the drag coefficient around N_{Re_c} but does not explain the subsequent rise in C_D in the supercritical regime.

A possible explanation is presented by Roshko for the case of a cylinder. He suggested that, in the supercritical range following first transition ($N_{Re} \doteq N_{Re_c}$) the boundary layer on the body undergoes laminar separation as at lower Reynolds numbers, transition to turbulence in the separated layer, reattachment of the fluid to the surface, and finally, turbulent separation. Thus a laminar separation bubble, as encountered on airfoils, may exist between the first separation and the surface of the body. Evidence of the possible existence of such a bubble on a sphere was first obtained by Fage (*18*), who observed a flat region in the pressure distribution on a sphere at the separation point. It is possible that a separation bubble exists in the supercritical regime from $N_{Re} \doteq N_{Re_c}$ up to what will be referred to as the *transcritical* Reynolds number N_{Re_T}, defined as that Reynolds number at which a maximum occurs in the $C_D - N_{Re}$ curve. This value of N_{Re} marks the beginning of the region that Roshko called the *transcritical regime* which is characterized by the disappearance of the separation bubble on the body.

The behavior of the wake in the Reynolds number range from N_{Re_c} to N_{Re_T} was deduced by Roshko from the form of the pressure distribution on a cylinder and the variation of Strouhal number with N_{Re}. He found that, in the lower transition (around N_{Re_c}), the wake width d_w decreased from values larger than the cylinder diameter d to values smaller than d. In the upper transition, or region of rising C_D, the wake reopened and d_w increased continuously up to N_{Re_T}, but never became larger than d. Since the pressure drag of a bluff body is determined primarily by the kinetic energy in the wake, it is clear that an increase in the size of this region causes a larger flow resistance. When the laminar separation bubble disappears, however, the separation is purely turbulent and any further displacement of the separation point is expected to be too slight to alter the drag significantly.

On the other hand, there is a strong probability that the shape of the $C_D - N_{Re}$ curves obtained at constant relative intensity of turbulence beyond the minimum C_D value, reflects a major change in the magnitude and relative contribution of the skin friction component of the total drag. It is well known that a flat plate undergoing transition experiences a large change in the skin friction coefficient C_f. Before this change, however, the skin friction of the laminar boundary layer reaches a minimum value which is considerably lower than that of a turbulent boundary layer at the same N_{Re}. For a sphere, this minimum C_f should coincide approximately with the minimum value of C_D determined largely by the extremely low value of the form drag. As N_{Re} is increased, however, an increased portion of the attached boundary layer becomes turbulent and with the higher value of C_f for a turbulent boundary layer, the total skin friction drag, based on the increased area, is bound to assume greater importance. The total drag thus increases up to N_{Re_T} where presumably the whole of the attached boundary layer has become turbulent. At N_{Re_T}, the separation is

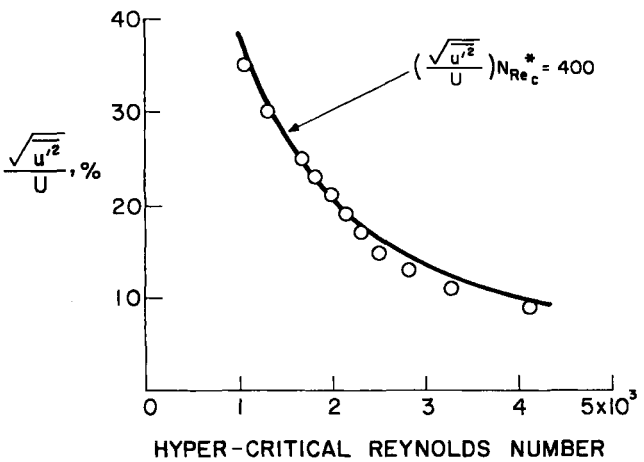

Fig. 4. Hypercritical Reynolds number of spheres as a function of relative intensity.

* Tabular material has been deposited as document NAPS-00280 with the ASIS National Auxiliary publications Service, c/o CCM Information Sciences, Inc., 22 W. 34th St., New York 10001 and may be obtained for $1.00 for microfiche or $3.00 for photocopies.

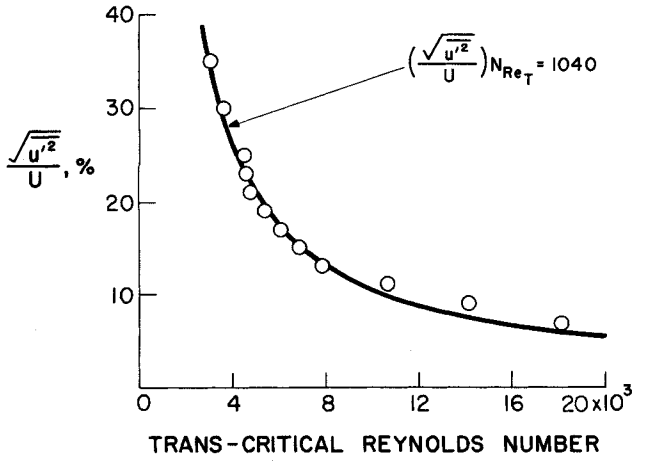

Fig. 5. Transcritical Reynolds number of spheres as a function of relative intensity.

purely turbulent and its position largely invariant. The drag coefficient from then on responds to the continuous decrease with N_{Re} of the skin friction coefficient for a turbulent layer. This trend has been observed for the turbulent boundary layer on a flat plate, and has been invoked by Hoerner (*8*) to predict a decrease in C_D for bluff bodies at $N_{Re} > N_{ReT}$. This hypothesis thus succeeds in explaining the variation of C_D with N_{Re} beyond the transcritical Reynolds number, which cannot be accounted for by Rosko's theory.

Regarding the influence of turbulence in this flow regime, it was shown qualitatively by Hoerner (*2*) that the supercritical drag on a sphere is increased by introducing turbulence into the flow. The effect of turbulence level on the critical Reynolds number N_{Rec}, which characterizes the lower transition, is well known. To determine the effect of free-stream turbulence on the upper transition, a new parameter known as the hypercritical Reynolds number $N_{Rec}{}^*$ was arbitrarily chosen to be that Reynolds number at which the rising portion of the $C_D - N_{Re}$ curve at constant intensity intersects the C_D value of 0.3. Values of $N_{Rec}{}^*$ for different intensities of turbulence are shown in Figure 4. The resulting curve was found to be well approximated, particularly at high relative turbulence intensities, by the following:

$$(\sqrt{\overline{u'^2}/U})\,(N_{Rec}{}^*) = 400 \qquad (6)$$

Another parameter which can be determined directly from the relative intensity of turbulence is the transcritical Reynolds number N_{ReT} (defined above). The functional relationship between N_{ReT} and I_R is shown in Figure 5 and can be expressed with reasonable accuracy by the following:

$$(\sqrt{\overline{u'^2}/U})\,(N_{ReT}) = 1{,}040 \qquad (7)$$

The above equations indicate a functional relationship resembling that obtained by Torobin and Gauvin (*1*) for the lowering of the critical Reynolds number N_{Rec} by free-stream turbulence. Confirmation has thus been provided to the suggested tendency that turbulence should also lower the critical values of N_{Re} associated with the upper transition.

The increase with intensity of the maximum values of C_D obtainable in the supercritical flow regime may be associated with the increased vorticity in the wake of a bluff body in the presence of free-stream turbulence. The direct effect of increasing intensities on the wake was found by Schubauer and Dryden (*6*) who observed the C_D for a flat plate set normal to the flow to increase gradually with turbulence intensity at a given N_{Re}. More recent experiments (*19, 20*) have shown that free-stream turbulence reduces the downstream extent of the near, or attached, wake by hastening the spatial return to free-stream conditions behind the particle. As the length of the wake decreases, the main flow is required to close more sharply behind the sphere. A greater lateral pressure gradient is then needed to produce the increased curvature of the streamlines, and, since the ambient free-stream pressure is fixed, there must be a decrease in the pressure at the rear of the particle and consequently an increase in drag.

The progressive decrease in the maximum value of C_D (at N_{ReT}) with decrease in intensity, which occurs at increasing values of N_{Re}, probably reflects a decrease in the value of the skin friction coefficient with increasing N_{Re}, thus providing additional evidence for the importance of the skin friction at very high Reynolds numbers.

The apparent lack of dependence of turbulence on C_D for spheres at these higher Reynolds numbers ($> N_{ReT}$), as reflected by the convergence of the various curves shown in Figure 3, is consistent with the views of earlier workers in this field (*4, 21, 22*) that turbulent skin friction is largely unaffected by the intensity of turbulence.

A generalized expression was found to predict, within about 15%, the variation of C_D with N_{Re} for the relative intensities of turbulence shown in Figure 3. For the range of I_R covered (7 to 35%) and for $N_{Rec}{}^* < N_{Re} < 3 \times 10^4$, the following equation may be used to determine C_D:

$$C_D = [3990/(\log N_{Re})^{6.10}] - [4.47 \times 10^5/(I_R)^{0.97} N_{Re}{}^{1.80}] \qquad (8)$$

From an examination of the data obtained it was apparent that the results were unaffected by the value of the scale ratio (L/D) in spite of the fact that there was an eightfold variation in this parameter. In addition, no effect of acceleration (or deceleration) was observed. The lack of dependence of momentum transfer on scale ratio or acceleration found in this study was also noticed by Torobin and Gauvin (*1*) in their study of the effects of turbulence on the drag coefficients of spheres. It would appear, then, that the effect of acceleration on the drag diminishes with increasing random vorticity in the wake and that the scale of turbulence plays a negligible or minor role in turbulent momentum transfer in the supercritical flow regime.

CONCLUSIONS

The development of suitable experimental techniques provided data of increased precision and made it possible to obtain reliable, quantitative measurements of the drag coefficients of single spherical particles moving in a turbulent air stream. Because of the range of Reynolds numbers and of turbulence intensities covered, the data obtained in this investigation extend farther into the supercritical flow regime than any other wind tunnel measurements previously reported in the literature. In particular, a maximum was observed, for the first time, in the $C_D - N_{Re}$ curve for spheres following transition.

From the shape of the drag curves obtained at constant relative intensity, it is apparent that the flow structure around a sphere changes continuously with increasing N_{Re} beyond the critical Reynolds number. Although any description of the alteration in particle flow field is pure conjecture at this time, the explanation of Roshko (*13*) regarding the change in flow pattern around a cylinder appears applicable to the sphere system. In addition, it is probable that skin friction may play an important part in determining drag coefficients for the turbulent boundary

layers at these large Reynolds numbers.

Functional relationships have been presented between the critical values of the Reynolds number associated with the various stages of the transition process, on the one hand, and the relative intensity of turbulence on the other. In general, the effect of turbulence is to increase supercritical drag, although this effect appears to diminish with increasing N_{Re} past the transcritical Reynolds number. Furthermore the maximum value of the drag coefficient obtainable in the supercritical flow regime is directly dependent upon the relative intensity of turbulence.

For the range of accelerations and turbulence scale ratios employed, no effect of either of these variables was found.

From a practical point of view, the data which have been presented should permit the calculation and prediction of particle trajectories and residence times in gas-solid or gas-liquid particulate systems, where the flow conditions are known or can be estimated, and where such complexities as particle-particle interactions or wall effects are negligible. The present results, together with those presented elsewhere (*1*), cover the flow conditions commonly met in most industrial applications such as pneumatic conveyors, spray-dryers, and transport reactors. Much work remains to be done to account for the many additional complexities which exist in industrial systems. Some of these have already been studied in these laboratories, such as the effects on the drag coefficient of acceleration and deceleration (*15*), particle shape (*15*), and simultaneous mass transfer (*23*).

ACKNOWLEDGMENT

We wish to express our appreciation to R. A. Lindsay for his valuable assistance in the development of the new particle tracking technique. Allen Clamen is indebted to the National Research Council of Canada for three consecutive fellowships in support of his research work.

NOTATION

A = frontal or wetted surface area, sq. ft.
A_p = projected area of sphere in direction of motion, $\pi D^2/4$, sq. ft.
a, b, c = constants in polynomial used to fit data
C_D = drag coefficient, $R/(1/2)\ (A_p\rho U^2)$, dimensionless
C_f = skin friction coefficient, $R_f/(1/2)\ (A\rho U^2)$, dimensionless
D = diameter of sphere, ft.
d = diameter of cylinder, ft.
d_w = wake diameter, ft.
E = absolute value of maximum possible error
g = acceleration due to gravity, ft./sq. sec.
I = intensity of turbulence, $\sqrt{\overline{u'^2}}/U_o$, dimensionless
I_R = relative intensity of turbulence, $\sqrt{\overline{u'^2}}/U$, dimensionless
K = empirical constant in Torobin and Gauvin's transition theory (*1*)
k = constant in Equation (5)
L = Eulerian macroscale of turbulence, ft.
m = mass of particle, lb.
N_{Re} = Reynolds number, $DU\rho/\mu$, dimensionless
N_{Rec} = critical Reynolds number for boundary layer transition
N_{Rec}^* = hypercritical Reynolds number, associated with rising portion of drag curve
N_{ReT} = transcritical Reynolds number, characterizing maximum in drag curve
N_{Sr} = Strouhal number, nD/U, dimensionless
n = frequency of wake shedding, $(\text{sec.})^{-1}$
R = fluid drag force on body, lb.$_f$
R_f = skin friction drag on body, lb.$_f$
R_y = Eulerian correlation coefficient, dimensionless
U = relative velocity between fluid and particle, ft./sec.
U_o = fluid velocity, ft./sec.
U_p = absolute velocity of particle, ft./sec.
U_p = acceleration rate of particle, ft./sq. sec.
u = instantaneous fluid velocity in x direction, ft./sec.
u' = fluctuating component of u, ft./sec.
x = direction component parallel to flow; length scale in direction of mean flow, ft.
y = direction component normal to flow and to bounding surface

Greek Letters

θ = time, sec.
λ = Eulerian microscale of turbulence, ft.
μ = dynamic viscosity, lb./(ft.)(sec.)
ρ = fluid density, lb./cu. ft.
ρ = particle density, lb./cu. ft.

LITERATURE CITED

1. Torobin, L. B., and W. H. Gauvin, *AIChE J.*, **7**, 615 (1961).
2. Hoerner, S. F., *Nat. Advisory Comm. Aeron. Memo 777* (1935).
3. Kline, S. J., A. V. Lisin, and B. A. Waitman, *Nat. Aeron. Space Admin. Tech. Note D-368* (1960).
4. Wadsworth, J., *Nat. Res. Council, Nat. Aeron. Estab. Rep. MT-39* (1958).
5. Ahlborn, F., *Z. Tech. Physik*, **12**, 10 (1931).
6. Schubauer, G. B., and H. L. Dryden, *Nat. Advisory Comm. Aeron. Rep. 546* (1935).
7. Jacobs, E. N., *Nat. Advisory Comm. Aeron. Tech. Note 312* (1929).
8. Hoerner, S. F., "Fluid Dynamic Drag", published by the author, Midland Park, N. J. (1958).
9. Relf, E. F., and L. F. G. Simmons, *Aeron. Res. Council (Gt. Brit.), Rep. Mem. 917* (1924).
10. Delany, N. K., and N. E. Sorensen, *Nat. Advisory Comm. Aeron. Tech. Note 3038* (1953).
11. Drescher, H., *Z. f. Flugwiss*, **4**, 17 (1956).
12. Fung, Y. C., J. *Aerospace Sci.*, **27**, 801 (1960).
13. Roshko, A., *J. Fluid Mech.*, **10**, 345 (1961).
14. Torobin, L. B., and W. H. Gauvin, *AIChE J.*, **7**, 406 (1961).
15. Marchildon, E. K., Ph.D. thesis, McGill Univ., Montreal (1965).
16. Clamen, A., R. A. Lindsay, and W. H. Gauvin, *J. Sci. Inst.*, to be published.
17. Lindsay, R. A., *ibid.*, to be published.
18. Fage, A., *Aeron. Res. Council (Gt. Brit.), Rep. Mem. 1766* (1936).
19. Eskinazi, S., *Nat. Aeron. Space Admin. Tech. Note D-83* (1959).
20. Eagleson, P. S., C. J. Huval, and F. E. Perkins, *Hydrodynamics Lab. Tech. Rep. 46*, Mass. Inst. Tech., Cambridge (1961).
21. Karlsson, S. K. F., *J. Fluid Mech.*, **5**, 622 (1959).
22. Abbott, D. E., and S. J. Kline, *J. Basic Eng.*, **84**, 317 (1962).
23. Clamen, A., and W. H. Gauvin, *Can. J. Chem. Eng.*, **46**, 73 (1968).

Manuscript received April 20, 1967; revision received January 29, 1967; paper accepted January 31, 1968.